Journal of Low Temperature Physics, Vol. 131, Nos. 5/6, June 2003 (© 2003)

A comparative study of MgB_2 and other diborides

G. Fuchs, S.-L. Drechsler, K.-H. Müller, A. Handstein, S.V. Shulga, G. Behr, A. Gümbel, J. Eckert, K. Nenkov, V.N. Narozhnyi, L. Schultz, H. Eschrig, S. Otani*, H. Rosner+, and W.E. Pickett+

Leibniz-Institut für Festkörper- und Werkstofforschung Dresden, P.O. Box 270116, D-01171 Dresden, Germany
**National Institute for Materials Science 1-2-1 Sengen, Tsukuba, Ibaraki 305-0047, Japan*
+Department of Physics, University of California, Davis, CA, 95616, USA

A combined experimental and theoretical study of superconducting, electronic and thermodynamic properties of various isomorphic diborides is reported. The $H_{c2}(T)$ data of bulk MgB_2 are analyzed within a two-band model with different couplings and Fermi velocities. No bulk superconductivity was found in TaB_2 and ZrB_2 single crystals at temperatures $T > 1.5$ K. Its absence is ascribed to weak electron-phonon coupling strenghth with $\lambda \sim 0.1$ derived both from the comparison of the calculated density of states at the Fermi level and specific heat data as well as from the weak deformation potential.
PACS numbers: 71.20 Lp, 74.25 Jb, 73.20 At, 74.60 Ec 74.60 Jg.

1. INTRODUCTION

The recent discovery of superconductivity in MgB_2[1] at temperatures as high as 40 K has stimulated broad activities including also other related diborides MB_2 (M = Li,Be,Al,Zr,Ta,Mo)[2–6]. Only few of them are superconductors. Contradictory results have been reported for TaB_2 and ZrB_2[5,6]. Superconductivity below T_c=9.5 K[5] and T_c=5.5 K[6] has been reported in TaB_2 and ZrB_2, respectively, whereas no superconductivity was found down to 1.5 K for TaB_2[7] and down to 1.8 K for ZrB_2[5]. The absence of superconductivity in TaB_2 was attributed to weak electron-phonon (el-ph) coupling[7], whereas a strong coupling scenario is necessary to explain the surprisingly high T_c of MgB_2. The upper critical field H_{c2}(T) plays a special role among the thermodynamic properties since it is most directly related to

0022-2291/03/0600-1159/0

the electronic structure via the Fermi-velocities of the most strongly coupled quasiparticles. The multi(two)-band nature of superconductivity in MgB_2 was put forward in Refs. 8-11. H_{c2}(T) of bulk MgB_2 will be analyzed in terms of such models taking into account the different couplings and of the Fermi velocities on different Fermi surface sheets. The usable H-T space for practical applications of MgB_2 is limited by the anisotropy of H_{c2}(T) and by the irreversibility line H_{irr}(T) which reaches, in bulk MgB_2, only 50 % of the upper critical field. In the present work data for nanocrystalline bulk MgB_2 with enhanced H_{irr}(T) will be presented. Furthermore, TaB_2 and ZrB_2 single crystals were studied both experimentally and theoretically by comparing their electronic structure with that of MgB_2.

2. SAMPLE PREPARATION AND MEASUREMENTS

Polycrystalline MgB_2 samples were prepared by a standard solid state reaction[13] and by mechanically alloying[14] resulting in bulk material with a grain size of 1-50 μm and 40-100 nm, respectively. For the mechanically alloyed material a MgB_2 phase fraction > 96 vol %, about 3 vol % MgO and about 0.3 vol % WC from the milling tools were found from x-ray diffraction. The MgB_2 samples were investigated by resistance and dc magnetization measurements in magnetic fields up to 16 T. TaB_2 and ZrB_2 single crystals prepared by the floating zone method[15,16] were investigated additionally by specific heat measurements. The orientation of single crystals was determined by the X-ray Laue back scattering method. Oriented samples for all measurements were prepared using a diamond wire saw.

3. RESULTS AND DISCUSSION

In Fig. 1 experimental H_{c2}(T) and H_{irr}(T) data of two MgB_2 samples prepared by sintering and by mechanical alloying are compared. The superconducting transition temperature, T_c , is 39 K for the sintered material, whereas a lower $T_c = 34.5$ K is found for the sample prepared by mechanical alloying. Despite of this lower T_c, the irreversibility line of the mechanical alloyed material is strongly shifted towards higher fields. Whereas typically $H_{irr} \sim 0.5\ H_{c2}$ is observed for sintered MgB_2 $H_{irr} \sim 0.8\ H_{c2}$ is found for the mechanical alloyed MgB_2. The improved pinning in this nanocrystalline material which is responsible for the enhanced irreversibility fields and the high critical currents ($j_c = 10^5 A/cm^2$ at 20 K and 1 T) is most probably due to the larger number grain boundaries compared to sintered samples with micrometer grain size. Furthermore, the nanocrystalline material shows a

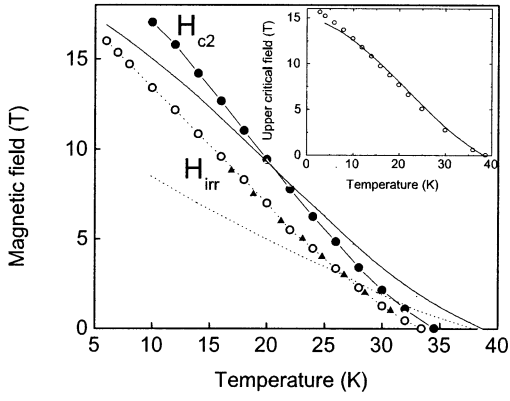

Fig. 1. $H_{c2}(T)$ (full lines) and $H_{irr}(T)$ (dotted lines) of two bulk MgB_2 samples prepared by sintering (no symbols) and by mechanical alloying (with symbols). Inset: Experimental data for H_{c2} of MgB_2 compared with the theoretical curve of the two-band model for both the different couplings and Fermi velocities (full line). Parameter set see Ref. 8.

slight increase of H_{c2} at low temperatures and has a ten times higher resisitivity $\rho(40\text{K}) = 46\ \mu\Omega$ cm than the sintered MgB_2 sample. The H_{c2}(T) curves in Fig. 1 show a positive curvature (PC) near T_c. It is more pronounced for the sintered than for the mechanical alloyed material. The PC cannot be explained within in the standard isotropic single band (ISB) model. Moreover, the ISB model would result in very low values of $H_{c2}(0) \sim 2$ T and cannot reproduce the magnitude of our data at low T shown in Fig. 1. These problems can be resolved within a two-band model[8,12] assuming two subgroups of quasiparticles with different Fermi velocities and el-ph coupling constants. These quantities were derived from the Fermi surface of MgB_2. The σ-tube Fermi surface sheets were chosen as the first effective band. The strong coupling in the heavy σ-bands combined with the weak coupling in the light π-band is responsible for the high values of $H_{c2}(0)$. An interband el-ph coupling and a weak interband impurity scattering included in the model ensure the PC of H_{c2}(T). The successfull description of experimental H_{c2}(T) data by the two-band model is illustrated in the inset of Fig. 1. TaB_2 and ZrB_2 single crystals of rod-shaped geometry (cross section 1-2 mm^2, length 3-5 mm) were investigated by resistance and dc magnetization measurements. No superconductivity was observed for both compounds for

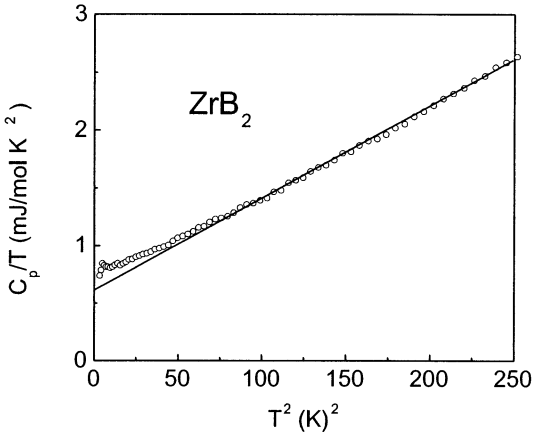

Fig. 2. Specific heat c_P(T)/T vs. T^2 of a ZrB_2 single crystal at zero magnetic field. The line correspond to linear regression fits of the experimental data for temperatures $T>$ 8 K.

$T > 1.5$ K. In Fig. 2 specific heat data are shown for ZrB_2. A Sommerfeld coefficient $\gamma = 0.68$ mJ/mol K^2 was found by extrapolating the straight line in Fig. 2 to $T = 0$. Sizable deviations of the experimental data from the linear fit observed in Fig. 2 at low T are ascribed to lattice effects related to boron disorder present in all diborides.

Band structure calculations were performed using the full-potential non-orthogonal local-orbital minimum-basis scheme within the local density approximation[7]. The calculated densities of states at the Fermi level, $N(\epsilon_F)$, the corresponding bare specific heat coefficients, γ_o, and the Sommerfeld coefficients are given in Table 1. Using these data, the el-ph coupling constants λ averaged over all Fermi surface sheets were determined from

$$\gamma = (\pi^2/3){k_B}^2(1+\lambda)N(\epsilon_F) = \gamma_o(1+\lambda). \qquad (1)$$

A very weak el-ph coupling ($\lambda\sim$ 0.1) is obtained for TaB_2 and ZrB_2. It differs significantly from the much stronger el-ph coupling for MgB_2 ($\lambda \sim 0.9$) caused by the strong coupling ($\lambda_\sigma \sim 1.3$) on in σ band derived hole tubes of the Fermi surface [18]. Our deformation potential calculations for the E_{2g}-mode [7] yield similar values $\approx$ 1 (MgB_2), 0.08 (ZrB_2), and 0.06 (TaB_2). Our LDA-FPLO calculations showed that TaB_2 and ZrB_2 differ from MgB_2 mainly by the absence/presence of σ bands, respectivelly. The weak el-ph

Table 1. Experimental and calculated data for TaB_2 and ZrB_2 single crystals. Resistivity ρ(300K) at 300 K, residual resistivity ratio, RRR, density of states at the Fermi level, $N(\epsilon_F)$ (in states/(eV cell)), bare specific heat coefficient γ_o, Sommerfeld coefficient γ, and el-ph coupling constants λ.

Sample	ρ(300K) [$\mu\Omega$cm]	RRR	$N(\epsilon_F)$	γ_o [mJ/(mol K^2)]	γ [mJ/(mol K^2)]	λ
TaB_2	67	1.2	0.91	2.14	2.3	0.07
ZrB_2	9	20	0.26	0.61	0.68	0.11

coupling found for ZrB_2 is in accord with small coupling constants derived from dHvA[18] and point-contact measurements[19] performed on samples obtained from the same single crystal. In view of this very weak el-ph coupling the absence of superconductivity in TaB_2 and ZrB_2 becomes very plausible.

ACKNOWLEDGMENTS

This research is supported by the DFG (MU 1015/8-1), the NSF-grant DMR-0114818 and the DAAD (H.R.).

REFERENCES

1. J. Nagamatsu, N. Hakagawa, T. Muranaka et al. *Nature* **410**, 63 (2001).
2. J.S. Slusky, N. Rogado, K.E. Regan et al. *Nature* **410**, 343 (2001).
3. I. Felner *Physica C* **353**, 11 (2001).
4. Y.G. Zhao, X.P. Zhang, P.Y. Qiao et al. cond-mat/0103077.
5. D. Kaczerowski, J. Klamut, and A.J. Zaleski, cond-mat/0104479.
6. Y.A. Gasparov, N.S. Sidorov et al. cond-mat/0104323.
7. H. Rosner, W.E. Picket, S.-L- Drechsler et al., *Phys. Rev. B* **64**, 144516 (2001).
8. S.V. Shulga, S.-L. Drechsler, H. Eschrig et al. cond-mat/01013154.
9. G. Fuchs, S.-L. Drechsler et al. in *Studies of High Temperature Superconductors* (Ed. A. Narlikar) Nova Science, New York, vol. **41**, p. 171 (2002) - in press.
10. A.Y. Liu, I.I. Mazin, and J. Kortus, *Phys. Rev. Lett.* **87**, 087005 (2001).
11. H.J. Choi, et al. *cond-mat*/0111182, *cond-mat*/0111183 (2001).
12. S.V. Shulga, S.-L. Drechsler, G. Fuchs et al., *Phys. Rev. Lett* **80**, 1730 [1998].
13. K.-H. Müller, G. Fuchs et al., *J.Alloys and Comp.* **322**, L10 (2001).
14. A. Gümbel, J. Eckert, G. Fuchs et al., *Appl. Phys. Lett.***80**, 2725 (2002).
15. S. Otani, M.M. Korsukova, T. Mitshhashi, *J. Crystal Growth* **194**, 430 (1998).
16. S. Otani et al. *J. Crystal Growth* **186**, 582 (1998).
17. S.L. Budko, C. Petrovic, G. Lapertot et al. *Phys. Rev. B* **63**, 220503 (2001).
18. S.-L. Drechsler, H. Rosner, J.M. Ann, et al., these Proceedings.
19. Y.G. Naidyuk, O.E. Kvinitskaya, I.K. Yanson, et al., *in preparation.*